ARTICLE

Excited State Intramolecular Proton Transfer of 1-Hydroxyanthraquinone

Si-mei Sun, Song Zhang*, Kai Liu, Ya-ping Wang, Miao-miao Zhou, Bing Zhang*

State Key Laboratory of Magnetic Resonance and Atomic and Molecular Physics, Wuhan Institute of Physics and Mathematics, Chinese Academy of Sciences, Wuhan 430071, China

(Dated: Received on April 20, 2015; Accepted on June 16, 2015)

The excited state intra-molecular proton transfer dynamics of 1-hydroxyanthraquinone in solution are investigated by femtosecond transient absorption spectroscopy and quantum chemistry calculations. Two characteristic bands of excited state absorption and stimulated emission are observed in transient absorption spectra with the excitation by the pump wavelength of 400 nm. From the delayed stimulated emission signal, the time scale of the intra-molecular proton transfer is determined to be about 32 fs. The quantum chemistry calculations show that the molecular orbits and the order of the S_2 and S_1 states are reversal and a conical intersection is demonstrated to exist along the proton transfer coordinate. After proton transfer, the second excited state of tautomer populated via the conical intersection undergoes the internal conversion with ∼200 fs and the following intermolecular energy relaxation with ∼16 ps. The longer component 300 ps can be explained in terms of the relaxation from excited-state tautomer to its ground state. From our observations, two proton transfer pathways via a conical intersection are proposed and the dominated one preserves the molecular orbits.

Key words: Proton transfer, Conical intersection, Transient absorption spectroscopy, 1-Hydroxyanthraquinone

I. INTRODUCTION

The transfer of a proton or a hydrogen atom from one group (-OH, -NH) to another (C=O, -N=) has been referred to as the most general and important reaction in chemistry and biology, such as acid-base neutralization and enzymatic reactions [1]. The excited state intramolecular proton transfer (ESIPT) processes belong to the fastest chemical reactions occurring in nature and are of a great interest from both the basic and applied points of view [2−4]. Over the past decades, the ESIPT processes have been studied and attracted much more attention due to the wide applications in luminescent materials, molecular memories and switches, proton transfer laser, photostabilizers, molecular probes, and metal ion sensors [3−15].

Anthraquinone and its derivatives are considered as the important molecules due to their structural similarity to both quinone antitumor drug and anthraquinoid vat dyes [16, 17]. 1-Hydroxyanthraquinone (1-HAQ) is the simplest anthraquinone derivative and an ideal model molecule for studying ESIPT processes. Extensive studies have been carried out to elucidate the intramolecular proton transfer [18−26]. In most cases, the ESIPT process involves a very low or negligible activation barrier, and hence, the process occurs with an exceptionally fast rate, typically on the subpicosecond time scale. On excitation in the near UV, two fluorescence bands of 1-HAQ can be observed, one with the usual resulting from an excited state (S_1(N)) of a normal structure and the other with a larger stokes shift originating from a proton-transferred state (S_1(T)) of a tautomeric [18]. The spectral features of the fluorescence excitation and emission spectra indicate that a significant change takes place in the intramolecular hydrogen bonding structure upon transition to the excited state, such as often seen in the excited state proton or hydrogen transfer [26]. Earlier, a simple four-state diagram has been proven to be a useful starting point for describing many facets of an ESIPT behavior [18−21]. However, there still exit other nonradiative decay processes accompanied by ESIPT, such as internal conversion (IC), intersystem crossing (ISC), intramolecular vibrational redistribution (IVR) and intermolecular energy relaxation (IER) [27−29]. Choi *et al.* determined that ESIPT of 1-HAQ occurs in 260 fs using transient absorption spectra and proposed that the time scales of 2 and 18 ps are assigned to an additional proton translocation introduced by IVR and the vibrational cooling process, respectively [22]. Afterwards, they reported that ESIPT was just 120 fs using fluorescence up-conversion with ∼250 fs cross-correlation by two-photon excitation [23]. In addition, the time scales of 2.5 and 18 ps were also obtained and different as-

*Authors to whom correspondence should be addressed. E-mail: zhangsong@wipm.ac.cn, bzhang@wipm.ac.cn, Tel.: +86-27-87198491, +86-27-87197441

signments were provided in comparison with transient absorption spectra. However, Ryu and his co-workers determined that ESIPT of 1-HAQ is only 45 fs using fluorescience up-conversion by two-photon excitation and the other components of ∼160 fs and 3.9 ps were not yet assigned and discussed [24]. In additional, the observed ns transient Raman results are discussed in relation to the reverse-ESIPT processes. However, the contributions of fluorescence with hundreds picosecond were mentioned in all the ultrafast experiments. Although the electronic ground state is predicted to be a single minimum potential along the reaction coordinate of tautomerization by *ab initio* calculations, it is unfortunately that the calculations on the excited states are rarely reported.

In this work, we employ femtosecond transient absorption spectroscopy combined with quantum chemical calculations to study ESIPT processes and the following ultrafast excited dynamics of 1-HAQ in solution. Two characteristic spectra bands were observed and analyzed in detail. We determined the time scale of ESIPT processes by the steplike emission rise and discussed the following ultrafast nonradiative processes via a conical intersection. Simultaneously, the quantum chemistry calculations are performed to predict the molecular orbits and energies of the excited states along the reaction coordinate. A more detailed and comprehensive schematic diagram is proposed and the whole excited state dynamics are reasonably described.

II. EXPERIMENTS AND COMPUTATION

Commercially available 1-HAQ (99% purity) was used without further purification. 1,4-Dioxane (99% purity) purchasing from Aladdin was used as solvent. A fresh sample was prepared for each measurement, and the concentration of 1-HAQ in 1,4-dioxane was 1 mmol/L at room temperature. The absorption spectra were recorded on a UV-Vis spectrophotometer (INESA, L6), and fluorescence spectra were recorded on a spectrometer (Princeton, SpectraPro 2500i) in a 1 mm quartz cell, respectively.

Ultrafast broadband transient absorption measurements were performed based on the Ti:sapphire femtosecond laser system. Details of the femtosecond laser system have been described elsewhere [30, 31]. Briefly, the seed beam is generated by a commercial Ti:sapphire oscillator pumped by a CW second harmonic of an Nd:YVO_4 laser, and then amplified by an Nd:YLF pumped regenerative amplifier to generate a 1-kHz pulse train centered at 800 nm of approximately 35-fs pulse width and with maximum energy of 1 mJ/pulse. The pump pulse of 400 nm is the second harmonic generation of the fundamental pulse obtained by a 0.5-mm-thick BBO crystal, with the energy ∼4 μJ at the sample position. A white light continuum generated by focusing the fundamental light on a 1-mm sapphire plate is reflected from the front and back surfaces of a quartz plate to obtain probe and reference beams. Both beams passed through the sample, and only the probe overlapped with the pump beam in the sample. The relative spot sizes of the pump and probe beams ensure that the focused probe light is homogeneously overlapped with the excitation pulses for the full spectral range of our experiment. The pump and probe pulses intersect in the sample at an angle of ∼4° and the relative polarization of the pump and probe pulses is set to the magic angle (54.7°) for all the measurements.

The absorbance of the sample solution is typically 1.0 at the excitation wavelength. The sample is circulated in a flow cell with two 1-mm thick CaF_2 windows and a 1-mm optical path length. 10000 laser shots are accumulated for each pump-probe delay. A linear translation stage is used to delay the probe beam in order to monitor the pump-probe dynamics. The resulting spectra are detected by a CCD camera (PI-MAX, 1024×256 pixel array) equipped with a spectrometer (Princeton, SpectraPro 2500i). The temporal dispersion of the white-light continuum for transient absorption spectra was corrected by nonresonant optical Kerr effect [32−35]. A polynomial fitting was used to obtain time-zero corrections at each wavelength. The instrumental response function of the system was estimated to be better than 150 fs.

The molecular orbitals of 1-HAQ were calculated using the B3LYP with 6-311G basis set. The geometries of the ground states of normal and tautomer forms were optimized using DFT and MP2 methods with different basis sets, respectively. All optimized geometries are confirmed to be stationary points by vibrational frequencies analysis. Vertical transition energies and oscillator strengths of the excited states were performed by TDDFT and CIS methods with several basis sets based on the optimized geometries of the ground states. Bulk solvent effects on the vertical excitation energies are considered by performing self-consistent reaction field calculation using the polarizable continuum model with the integral equation formalism. All quantum chemical calculations are carried out using the Gaussian 09W suit of program [36]. The data analysis is achieved by a global analysis method that uses a singular value decomposition (SVD) method to reduce the size of the fitted data [35, 37−39]. Global analysis of the data was performed to determine the sufficient number of decay components and obtain the decay-associated difference spectra (DADS). A series of models were applied when the decay lifetimes were obtained, and the goodness of the fit was judged using the value of root-mean-square error.

III. RESULTS AND DISCUSSION

A. Static absorption and transient absorption spectra

The steady UV-Vis absorption and fluorescence spectra of 1-HAQ are depicted in Fig.1. As can be seen, the

DOI:10.1063/1674-0068/28/cjcp1504078

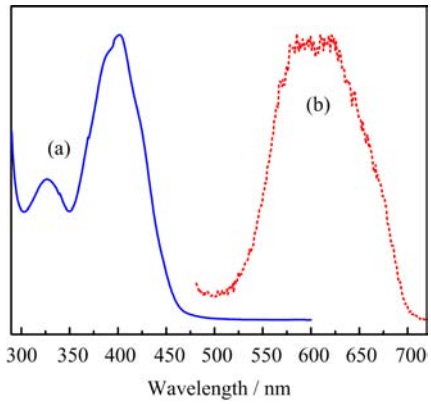

FIG. 1 (a) UV-Vis steady absorption and (b) fluorescence spectra with the excitation at 400 nm in 1,4-dioxane.

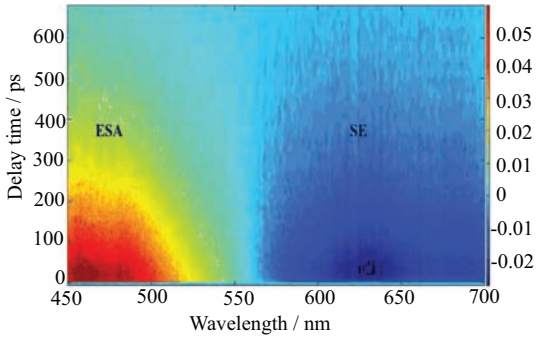

FIG. 2 Transient absorption spectra of 1-HAQ in 1,4-dioxane with the excitation at 400 nm. Two characteristic spectra bands are presented: stimulated emission (SE) and excited state absorption (ESA).

absorption spectrum at the wavelengths of >300 nm reveals three broad and distinguishable absorption bands. A relative much stronger absorption band is peaked at 400 nm. Following an excitation at 400 nm, a strongly red shifted and broad emission is observed. An enormously large Stokes shifted band is located at 625 nm and the other relatively weaker emission is at a wavelength shorter than 500 nm. The calculated vertical excitation energies of the excited states of the normal form at several methods with different basis sets are listed in Table I. In our calculations, the tautomer structure is verified to be unstable in the S_0 state and always converges to the normal one. For a normal structure, all calculations reveal that the lowest excited S_1 state is forbidden and originates a 59←57 transition, whereas the second excited S_2 state originates a 59←58 transition and has a large transition dipole moment. The 57 and 58 orbits are the HOMO-1 and HOMO, respectively, and orbits in the Franck-Condon region, whereas the 59 orbit is the LUMO and belongs to a π^* orbit. The original transition to the first populated excited state of jet-cooled 1-HAQ was determined to be at 461.98 nm using laser induced fluorescence and resonant $1+1'$ ionization [26]. The calculated vertical excitation energies of the S_2 state are close to the transition to the first optical populated state of jet-cooled 1-HAQ.

The pump wavelength is 400 nm and coincides with the peak of the $\pi\pi^*$ absorption band of the molecules. The transient absorption spectra of 1-HAQ in 1,4-dioxane are measured from 450 nm to 700 nm, as shown in Fig.2. It obviously divides into two main broad bands. The region at wavelength <560 nm is a positive signal and elucidated by the excited state absorption (ESA). And the other region from 560 nm to 700 nm is a negative signal and originated from the stimulated emission (SE).

To properly describe the dynamics observed in the visible range, global fit analysis of all of the kinetics at different wavelength regions is performed with singular value decomposition (SVD). Decay-associated difference spectra (DADS) are obtained from the global analysis, as shown in Fig.3. The two fast components originate from the decay of the same state since their spectral shapes are similar. The amplitudes of two fast components are opposite to those of the slow component. And the weights of the slow component are the main contribution because its amplitude is obviously larger than others. The best fit results of the decay time are listed in Table II. Several typical wavelengths 456 and 487 nm, and 633 and 687 nm are chosen to represent the temporal behavior of ESA and SE bands, respectively, shown in Fig.4. The global analysis result shows a good match with the experimental traces over the whole spectra-temporal range.

TABLE I Vertical excitation energies E_v and oscillator strengths f of 1-HAQ in 1,4-dioxane calculated with different methods.

Method	S_1		S_2	
	E_v/eV	f	E_v/eV	f
B3LYP/6-311G	2.8711	0	2.9530	0.1780
B3LYP/Lanl2dz	2.8199	0	2.9583	0.1822
B3PW91/6-311G	2.8506	0	2.9618	0.1797
B3PW91/Lanl2dz	2.7980	0	2.9727	0.1848
PBEPBE/6-311G	2.2679	0	2.5243	0.1346
PBEPBE/Lanl2dz	2.1965	0	2.5256	0.1330
CCSD/6-311G	4.2629	0	4.3892	0.5436
CIS/6-311G	4.2625	0	4.3894	0.5438
CIS/Lanl2dz	4.2384	0	4.4010	0.5552
Expt.			2.68 [26]	

B. Excited state intramolecular proton transfer

The $S_2(\pi\pi^*)$←S_0 transition of 1-HAQ exhibits a maximum absorptivity and emission around 400 and 625 nm, respectively. The large Stokes shift of ∼9000 cm^{-1} appears between the absorption and fluorescence bands. The significantly large width of the

DOI:10.1063/1674-0068/28/cjcp1504078

TABLE II Results of the global fit analysis of the absorption-time profiles of 1-HAQ in 1,4-dioxane. Values in parentheses give the 2σ standard deviations with respect to the last digits.

λ/nm	a_1	τ_1/ps	a_2	τ_2/ps	a_3	τ_3/ps
464	−0.050(8)	0.238(5)	−0.066(2)	16(3)	0.516(16)	300(5)
476	−0.031(4)	0.238(5)	−0.039(2)	16(3)	0.326(4)	300(5)
488	−0.040(4)	0.238(5)	−0.041(1)	16(3)	0.327(7)	300(5)
500	−0.061(5)	0.238(5)	−0.024(1)	16(3)	0.298(9)	300(5)
630	0.045(6)	0.238(5)	0.063(4)	16(3)	−0.205(13)	300(5)
648	0.050(4)	0.238(5)	0.060(1)	16(3)	−0.185(1)	300(5)
666	0.045(6)	0.238(5)	0.070(6)	16(3)	−0.188(16)	300(5)
685	0.045(4)	0.238(5)	0.062(1)	16(3)	−0.161(1)	300(5)

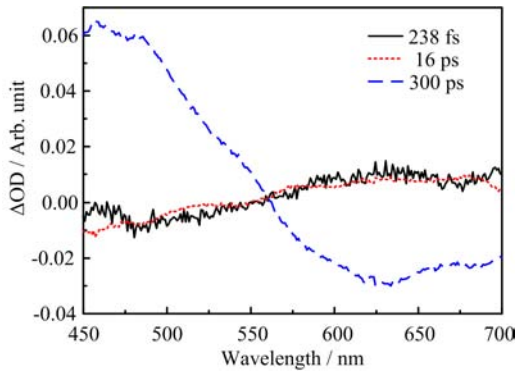

FIG. 3 Decay-associated difference spectra from global fit analysis with predominantly three components.

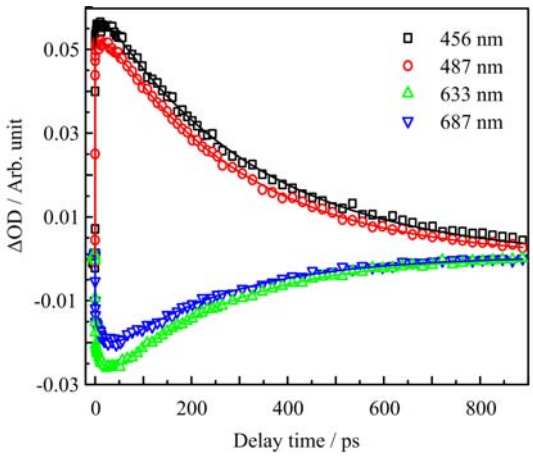

FIG. 4 Kinetic traces of the transient absorption spectra of 1-HAQ at several probe wavelengths.

emission compared to the absorption band clearly indicates that the molecule has undergone a significant rearrangement, in this case the proton transfer. The strong and large Stokes shifted band at 625 nm is the tautomer emission from ESIPT whereas the weaker band at <500 nm is assigned to the normal-form. It is suggested that the "dual emission" is a telltale sign of ESIPT in anthraquinone compounds [18−20]. As mentioned above, the tautomer structure is unstable in the S_0 state and converges to the normal one. After an excitation, hydrogen atom in hydroxyl group of the normal form transfers to the anthraquinone oxygen atom on the excited potential surface. Figure 5(a) shows the time-resolved transient absorption spectra of 1-HAQ at the first 300 fs delay times. The ESA signal rapidly appears whereas the SE signal is absent until tens of femtosecond. After the excitation, a rise of the SE band is observed with a small but finite delay, shown in Fig.5(b). The fitted delay of the step like emission rise as a function of the probe wavelength is determined to be 32 fs. The inserted curves in Fig.5(b) show the time-resolved kinetic traces of 1-HAQ at four probe wavelengths within the first 2 ps after the excitation. The dominant feature is that there emerges a time delay of <40 fs in the rising of SE band above 560 nm compared with ESA. The delayed emission observed in our measurements can safely be associated with the appearance of the products of the ESIPT form. Taking into regard the ∼150 fs width of the instrumental function, this time is beyond the temporal resolution of our apparatus. In *o*-hydroxybenzaldehyde and 2-(2′-hydroxyphenyl) benzothiazole, the delayed rise of SE signal were also observed and assigned to the ESIPT processes [40, 41]. ESIPT of 1,8-DiHAQ is estimated less than 55 fs by femtosecond time-resolved fluorescence spectroscopy [42]. Furthermore, ESIPT of 1-HAQ is also determined to be 45 fs by fluorescence up-conversion [24].

Electronic spectroscopy of 1-HAQ also indicates that the transition to the excited state accompanies a large structural change in the intramolecular hydrogen bond [26]. The vibrational progression in the excitation spectrum and the large Stokes shifted emission result from the distortion of the intramolecular hydrogen bond through active coupling of vibrations related to O−H stretching motion. In addition, the O−H stretching vibration is at 2940 cm^{-1} to the red of the original band in the emission spectra and can be directly excited by the pump pulse in Franck-Condon region. The directly exited O−H stretching mode is devoted to ultrafast ESIPT.

DOI:10.1063/1674-0068/28/cjcp1504078

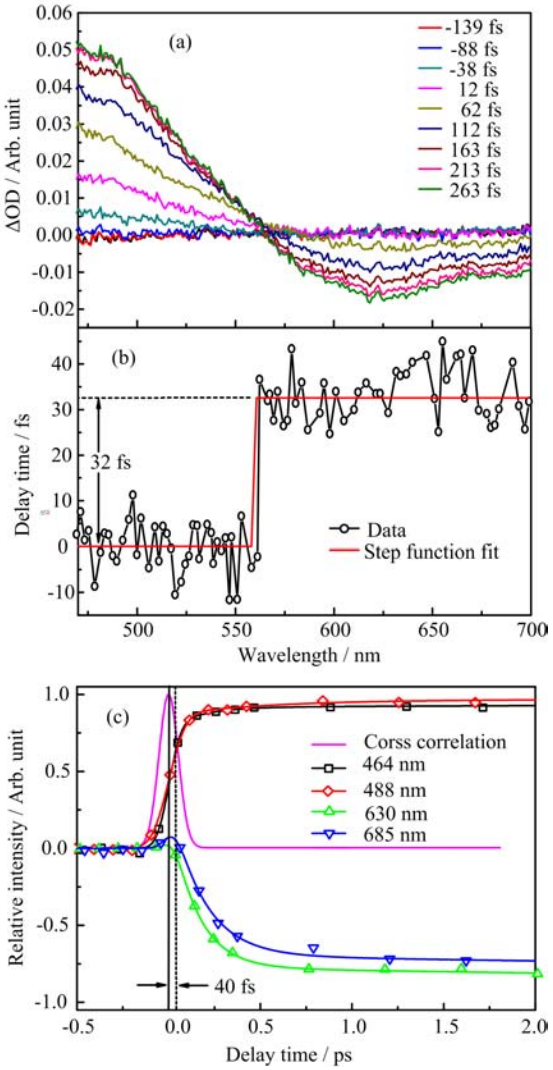

FIG. 5 (a) Time-resolved transient absorption signals of 1-HAQ at early 300 fs. (b) Fitted delay of the steplike emission rise relative to the absorption signal as a function of the probe wavelength. (c) Time-resolved kinetic traces of 1-HAQ at four probe wavelengths within the first 2 ps.

C. Following nonradiative relaxation

The energies of the two lowest excited states of a tautomer are also performed at the same methods based on the optimized geometry of the S_2 state of the tautomer structure, listed in Table III. It is noticed that the energies of 59←58 and 59←57 transitions are located at 2.9727 and 2.7980 eV in the normal form and 2.3842 and 2.5180 eV in the tautomer form, respectively. The 59←58 and 59←57 transitions of the tautomer structure are redefined as the S'_1 and S'_2 states, respectively. It is obviously that the S_2 and S'_1 states, or the S_1 and S'_2 states are the same orbits, respectively. The energies of both transitions are reverse along the proton transfer pathway.

A simple four-state diagram has previously proven to

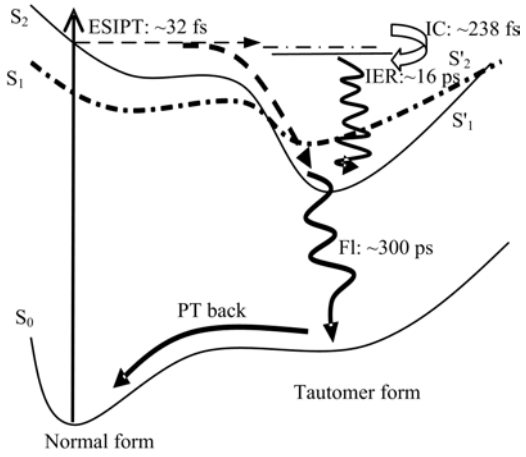

FIG. 6 Schematic diagram of electronic energies and proposed decay of the excited states of 1-HAQ. ESIPT: excited state intramolecular proton transfer, IC: internal conversion, IER: intermolecular energy relaxation, FL: fluorescence, PT back: proton transfer back from the tautomer-form to the normal-form.

be a useful starting point for describing many facets of ESIPT behavior [18−20]. However, our calculations show that the excitation to the S_1 state is forbidden but allowed to the S_2 state. Therefore, more than two excited states should be associated with the ESIPT process. The simple four-state diagram is not reasonable to depict the whole ultrafast dynamics including the ESIPT and the following nonradiative decay processes. Our calculations also verify that the energies of the lowest two excited states are reversal at the normal and tautomer structures. Simultaneously, the molecular orbits are also exchanged each other. Along the ESIPT coordinate, there exists a conical intersection between the potential surfaces of the two excited states, shown in Fig.6. Two proton transfer pathways are proposed in the excited states after photoexcitation. One is that the S_2 state directly transfers into the S'_1 state of tautomer via a conical intersection and preserves the original molecular orbits. The other is that the S_2 state adiabatically transfers to the S'_2 state of tautomer with the reverse of molecular orbits. After proton transfer, the S'_2 state of tautomer decays to the high vibrational S'_1 state by an internal conversion with ∼200 fs. Our theoretical approaches indicate that the tautomer form is higher 0.25 eV (2016 cm^{-1}) than the normal form in the ground states. Adding the absorption maximum of 400 nm (25000 cm^{-1}) for the S_2←S_0 ($\pi\pi^*$) energy gap of the normal-form and the emission maximum of 625 nm (16000 cm^{-1}) for the S'_1→S'_0 energy gap of the tautomer-form, the energy of the S_2 state of the normal form is qualitatively estimated to be ∼7000 cm^{-1} above that of the S'_1 state of the tautomer form. Afterwards, the high vibrational S'_1 state decays by the intermolecular energy relaxation with ∼16 ps. Through a fast S'_2→S'_1 internal conversion, this amount of energy is re-

DOI:10.1063/1674-0068/28/cjcp1504078

TABLE III Vertical energies E of the two lowest singlet states before and after ESIPT process using B3PW91/Lanl2dz, respectively.

Normal form			Tautomer form		
State	Transition	E/eV	State	Transition	E/eV
S_0		0	S_0'		0.2501
S_1	59←57	2.7980	S_1'	59←58	2.3842
S_2	59←58	2.9727	S_2'	59←57	2.5180

distributed over many vibrational modes during the motion of the system on the excited-state potential surface resulting in a vibrationally hot molecule, which then cools by collisions with the surrounding solvent.

Recently the intermolecular energy relaxation is found to occur on the time scale of <100 ps by collisional interaction with solvent molecules [43−49]. Intramolecular vibrational energy redistribution was concluded to a subpicosecond process while the intermolecular energy relaxation process is an order of magnitude slower. And the authors also concluded that the cooling of the molecules by interaction with the solvent is monitored via the thermal broadening of the emission spectrum and shows a distinctly kinetics of 1−50 ps with solvent dependence. In our experiments, the broadening in emission band is also observed, show in Fig.5(a). The decay time τ_3 is assigned to the lifetime of the S_1' state with 300 ps in ESA band and 250 ps in SE band, respectively, and in good agreement with previous values obtained by time-resolved spectra [22−25]. The difference of the lifetimes between ESA and SE bands may be derive from the intersystem crossing to the triplets. The pre-exponential factors of the component τ_3 are opposite to that of the other two components τ_1 and τ_2 at the all selected wavelengths. Furthermore, the amplitudes of components τ_3 are almost average 3−10 times larger than others at the selected wavelengths. It suggests that the transfer from the S_2 state to the S_1' state is dominated and contributes mostly to the components τ_3 because both states maintain the same orbits. And the other shorter components derive from the pathway from the S_2 state to the S_2' state and are attributable to a small ratio of the component τ_3 via the adiabatic pathway. Our calculations predict that the structure of the ground state of the tautomer form is unstable and always converges to the normal form at the DFT level. Finally, the tautomer goes back to the initial structure on a barrierless potential curve.

IV. CONCLUSION

The ESIPT and following ultrafast excited state dynamics of 1-HAQ in 1,4-dioxane were studied in detail by ultrafast time-resolved absorption spectroscopy combined with quantum chemical calculations. Two main absorption bands were illustrated by the excitation at 400 nm to the S_2 state. The ESIPT process was observed and determined to be about 32 fs by the delayed SE signal. The calculations demonstrate that the order of the S_2 and S_1 states is reversal and a conical intersection is formed along the evolution of the ESIPT coordinate. The populated S_2' state through the conical intersection undergoes IC with a time of 238 fs and a following solvent related intermolecular energy relaxation with a time of ∼16 ps. The transfer to the S_1' state is dominated due to the consistency of orbits. The S_1' state relaxes to its corresponding ground state with a decay of 300 ps. Finally, the proton transfer goes back to the ground state of the normal-form from the tautomer-form. Based on the novel experimental and computational data, we suggested a more detailed diagram in interpreting the ESIPT process and the following excited state dynamics.

V. ACKNOWLEDGMENTS

This work was supported by the National Basic Research Program of China (No.2013CB922202) and the National Natural Science Foundation of China (No.11174328, No.21273274, No.21173256, No.91121006, and No.21203241).

[1] E. F. Caldin and V. Gold, *in: Proton-transfer Reactions*, London: Chapmann and Hall, (1975).
[2] T. Elsaesser and H. J. Bakker, *Ultrafast Hydrogen Bonding Dynamics and Proton Transfer Processes in the Condensed Phase*, Dordrecht: Kluwer Academic Publishers, (2002).
[3] M. Chattoraj, B. A. King, G. U. Bublitz, and S. G. Boxer, Proc. Natl. Acad. Sci. **93**, 8362 (1996).
[4] C. Fang, R. R. Frontiera, R. Tran, and R. A. Mathies, Nature **462**, 200 (2009).
[5] J. E. Kwon and S. Y. Park, Adv. Mater. **23**, 3615 (2011).
[6] M. Irie, Chem. Rev. **100**, 1683 (2000).
[7] K. Y. Chen, C. C. Hsieh, Y. M. Cheng, C. H. Lai, and P. T. Chou, Chem. Commun. **41**, 4395 (2006).
[8] J. Keck, H. E. A. Kramer, H. Port, T. Hirsch, P. Fischer, and G. J. Rytz, Phys. Chem. **100**, 14468 (1996).
[9] J. Wu, W. Liu, J. Ge, H. Zhang, and P. Wang, Chem. Soc. Rev. **40**, 3483 (2011).
[10] M. Taki, J. L. Wolford, and T. V. O'Halloran, J. Am. Chem. Soc. **126**, 712 (2004).
[11] R. Vivie-Riedle, V. D. de Waele, L. Kurtz, and E. Riedle, J. Phys. Chem. A **107**, 10591 (2003).
[12] S. Takeuchi and T. Tahara, J. Phys. Chem. A **109**, 10199 (2005).
[13] C. H. Kim and T. Joo, Phys. Chem. Chem. Phys. **11**, 10266 (2009).
[14] C. Schriever, S. Lochbrunner, A. R. Ofial, and E. Riedle, Chem. Phys. Lett. **503**, 61 (2011).
[15] J. Lee, C. H. Kim, and T. Joo, J. Phys. Chem. A **117**, 1400 (2013).

DOI:10.1063/1674-0068/28/cjcp1504078

[16] J. W. Lown, *Anthracycline and Anthracencedione-based Anticancer Agents*, Amsterdam: Elsevier, (1988).
[17] M. W. Rembold and H. E. A. Karmer, J. Soc. Dyers Colour. **96**, 122 (1980).
[18] S. Nagaoka and U. Nagashima, Chem. Phys. **206**, 353 (1996).
[19] T. P. Smith and K. A. Zaklika, J. Phys. Chem. **95**, 10465 (1991).
[20] T. P. Smith and K. A. Zaklika, J. Am. Chem. Soc. **113**, 4035 (1991).
[21] M. H. V. Benthem and G. D. Gillispie, J. Phys. Chem. **88**, 2954 (1984).
[22] J. R. Choi, S. C. Jeoung, and D. W. Cho, Bull Korean Chem. Soc. **24**, 1675 (2003).
[23] J. R. Choi, S. C. Jeoung, and D. W. Cho, Chem. Phys. Lett. **385**, 384 (2004).
[24] J. Ryu, H. W. Kim, M. S. Kim, and T. Joo, Bull Korean Chem. Soc. **34**, 465 (2013).
[25] K. Gollnick, S. Held, D. O. Mrtire, and S. E. Braslavsky, J. Photochem. Photobiol. A **69**, 155 (1992).
[26] S. H. Cho, H. Huh, H. M. Kim, C. I. Kim, N. J. Kim, and S. K. Kim, J. Chem. Phys. **122**, 034304-8 (2005).
[27] P. T. Chou, Y. C. Chen, W. S. Yu, Y. H. Chou, C. Y. Wei, and Y. M. Cheng, J. Phys. Chem. A **105**, 1731 (2001).
[28] M. N. Khimich, V. A. Nadtochenko, L. D. Popov, A. S. Burlov, V. L. Ivanov, N. N. Denisov, F. E. Gostev, I. V. Shelaev, O. M. Sarkisov, and B. M. Uzhinov, High Energy Chem. **46**, 247 (2012).
[29] D. Shemesh, A. L. Sobolewski, and W. Domcke, J. Am. Chem. Soc. **131**, 1374 (2009).
[30] S. Sun, S. Zhang, K. Liu, Y. Wang, and B. Zhang, Photochem. Photobiol. Sci. **14**, 853 (2015)
[31] Y. Wang, S. Zhang, S. Sun, K. Liu, and B. Zhang, Chin. J. Chem. Phys. **26**, 651 (2013).
[32] S. Yamaguchi and H. Hamaguchi, Appl. Spectro. **49**, 1513 (1995).
[33] D. H. Quan, S. L. Liu, L. Zhang, J. Yang, L. Wang, G. Z. Yang, and Y. X. Weng, Chin. Phys. **12**, 986 (2003).
[34] A. Buzády, J. Savolaimen, J. Erostyák, P. Myllyperkiö, B. Somogyi, and J. Korppi-Tommola, J. Phys. Chem. B **107**, 1208 (2003).
[35] D. Zhou, E. Mirzakulova, R. Khatmullin, I. Schapiro, M. Olivucci, and K. D. Glusac, J. Phys. Chem. B **115**, 7136 (2011).
[36] M. J. Frisch, G. W. Trucks, H. B. Schlegel, G. E. Scuseria, M. A. Robb, J. R. Cheeseman, G. Scalmani, V. Barone, B. Mennucci,G. A. Petersson, H. Nakatsuji, M. Caricato, X. Li, H. P. Hratchian, A. F. Izmaylov, J. Bloino, G. Zheng, J. L. Sonnenberg, M. Hada, M. Ehara, K. Toyota, R. Fukuda, J. Hasegawa, M. Ishida, T. Nakajima, Y. Honda, O. Kitao, H. Nakai, T. Vreven, J. A. Jr. Montgomery, J. E. Peralta, F. Ogliaro, M. Bearpark, J. J. Heyd, E. Brothers, K. N. Kudin, V. N. Staroverov, R. Kobayashi, J. Normand, K. Raghavachari, A. Rendell, J. C. Burant, S. S. Iyengar, J. Tomasi, M. Cossi, N. Rega, J. M. Millam, M. Klene, J. E. Knox, J. B. Cross, V. Bakken, C. Adamo, J. Jaramillo, R. Gomperts, R. E. Stratmann, O. Yazyev, A. J. Austin, R. Cammi, C. Pomelli, J. W. Ochterski, R. L. Martin, K. Morokuma, V. G. Zakrzewski, G. A. Voth, P. Salvador, J. J. Dannenberg, S. Dapprich, A. D. Daniels, Ö. Farkas, J. B. Foresman, J. V. Ortiz, J. Cioslowski, and D. J. Fox, G*aussian 09, Revision A02*, Wallingford CT: Gaussian, Inc., (2009).
[37] W. G. Chen and M. S. Braiman, Photochem. Photobiol. **54**, 905 (1994).
[38] S. Yamaguchi and H. Hamaguchi, J. Chem. Phys. **109**, 1397 (1998).
[39] J. P. Zhang, T. Inaba, Y. Watanabe, and Y. Koyama, Chem. Phys. Lett. **331**, 154 (2000).
[40] K. Stock, T. Bizjak, and S. Lochbrunner, Chem. Phys. Lett. **354**, 409 (2002).
[41] S. Lochbrunner, A. J. Wurzer, and E. Riedle, J. Chem. Phys. **112**, 10699 (2000).
[42] S. Y. Arzhantev, S. Yakeuchi, and T. Tahara, Chem. Phys. Lett. **330**, 83 (2000).
[43] A. Mokhtari, J. Chesnoy, and A. Laubereau, Chem. Phys. Lett. **155**, 593 (1989).
[44] W. Wild, A. Seilmeier, N. H. Gottfried, and W. Kaiser, Chem. Phys. Lett. **119**, 259 (1985).
[45] Y. Mizutani, Y. Uesugi, and T. Kitagawa, J. Chem. Phys. **111**, 8950 (1999).
[46] T. Elsaesser and W. Kaiser, Annu. Rev. Phys. Chem. **42**, 83 (1991).
[47] T. Sekikawa, T. Kobayashi, and T. Inabe, J. Phys. Chem. A **101**, 644 (1997).
[48] S. Takeuchi and T. Tahara, J. Phys. Chem. A **102**, 7740 (1998).
[49] T. Fiebig, M. Chachisvillis, M. Manger, A. H. Zewail, A. Douhal, I. Garcia-Ochoa, and A. de La Hoz Ayuso, J. Phys. Chem. A **103**, 7419 (1999).

DOI:10.1063/1674-0068/28/cjcp1504078